

Supplementary Information. Harnessing the polymer-particle duality of ultra-soft nanogels to stabilise smart emulsions

Alexander V. Petrunin, Steffen Bochenek, Walter Richtering, and Andrea Scotti
Institute of Physical Chemistry, RWTH Aachen University, 52056 Aachen, Germany, EU
(Dated: August 26, 2022)

I. DYNAMIC LIGHT SCATTERING

Swelling curves of the ULC nanogels and nanogels that have been synthesised adding 1 and 2.5 mol% of crosslinker (BIS) are shown in Figure S1. The volume phase transition that leads to a dramatic decrease in size occurs at 31-32 °C for ULC and 2.5 mol% BIS nanogels and at 33 °C for 1 mol% BIS nanogels. The shift of VPTT in the latter case is due to the presence of comonomer APMH, which can decrease the hydrophobic hydration of pNIPAM [1]. All radii in Figure S1 are normalized to the collapsed state ($T = 50$ °C), so that the swelling degree is readily available from the curves. The exact values of swollen and collapsed hydrodynamic radii of the nanogels can be found in Table I.

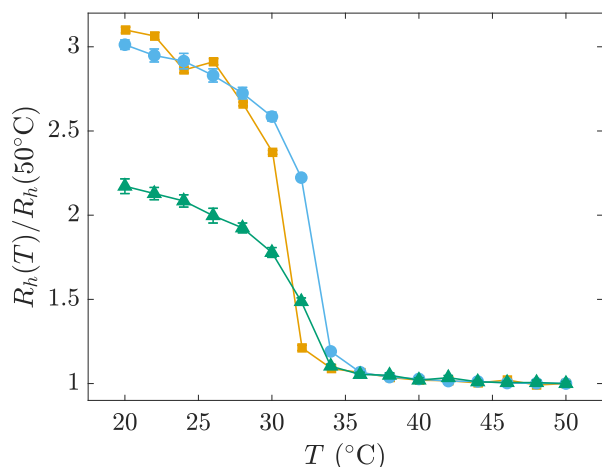


FIG. S1: Hydrodynamic radii normalised to the collapsed state as a function of temperature for ULC nanogels (orange squares), 1 mol% BIS nanogels (blue circles), and 2.5 mol% BIS nanogels (green triangles).

Swelling equilibrium of neutral nanogels results from the balance between the free energies due to the polymer-solvent mixing and due to the elastic energy of the network [2]. The higher amount of crosslinker agent used during the synthesis results in higher stiffness of the network [3], whereas the mixing contribution depends only on the Flory solvency parameter [4, 5] of pNIPAM in water. Therefore, 2.5 mol% BIS nanogels swell much less below the VPTT with respect to 1 mol% BIS and ULC nanogels. Interestingly, 1 mol% and ULC nanogels show almost identical swelling degrees defined as $R_h(20^\circ\text{C})/R_h(50^\circ\text{C})$. This means that the two

nanogels have comparable softness as a result of a very few crosslinks within the network [3, 6]. However, 1 mol% BIS nanogels have been reported to have a more pronounced core-corona structure [7] because of higher reactivity of the crosslinker [8], whereas the ULC nanogels have a more homogeneous internal structure as revealed by small-angle neutron scattering [7] and atomic force microscopy in force volume mode measurements [9]. This structural difference results in a higher deformability of ULC nanogels and a peculiar disk-like shape upon adsorption at interfaces [9].

II. STATIC LIGHT SCATTERING

Figure S2 shows the Zimm plot [10] for linear pNIPAM, from which the molecular weight, $M_w = (1.9 \pm 0.5) \cdot 10^5$ g/mol, and the second virial coefficient, $A_2 = (1.3 \pm 0.1) \cdot 10^{-3}$ mol·mL/g², were determined.

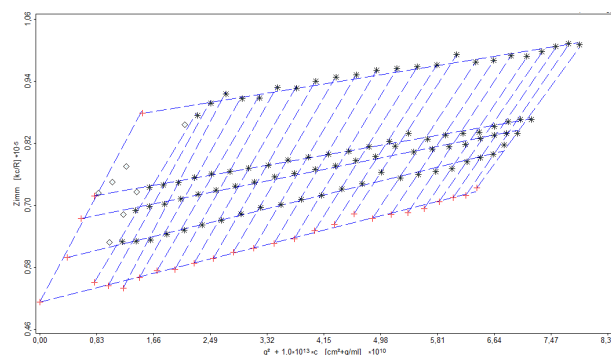


FIG. S2: Zimm plot from static light scattering of linear pNIPAM.

III. CAPILLARY VISCOMETRY

Dynamic viscosity of a suspension of spherical particles in dilute conditions is connected to their volume fraction, ϕ , by the Einstein-Batchelor equation: $\eta/\eta_s = 1 + 2.5\phi + 5.9\phi^2$, where η_s is the viscosity of water. In case of soft particles like nanogels that can deswell and deform, the generalised volume fraction, ζ , is commonly used instead of ϕ [11–13]. The generalised volume fraction expresses the volume occupied by the particles in solution assuming that their volume is the fully-swollen

state and is proportional to the weight fraction, c :

$$\zeta = \frac{Nv_{sw}}{V_{tot}} \approx \frac{\rho_s v_{sw}}{\rho_{pol} v_{dry}} \cdot \frac{m_{pol}}{m_{tot}} = k \cdot c \quad (S1)$$

where N is the number of nanogels in suspension, V_{tot} is the total volume of the suspension, m_{tot} is the total mass of the suspension, v_{sw} and v_{dry} are the volumes of a fully-swollen and dry nanogel particle, respectively, ρ_{pol} and ρ_s are the densities of polymer and solvent, respectively, and k is the conversion constant.

At low concentrations, $\phi = \zeta$ that gives:

$$\frac{\eta}{\eta_s} = 1 + 2.5(kc) + 5.9(kc)^2 \quad (S2)$$

Figure S3 shows the relative viscosities $\eta_r = \eta/\eta_s$ vs. c of ULC and BIS-crosslinked nanogels in suspension. The smaller the crosslinker content, the steeper the relative viscosity increases with concentration. ULC nanogels have the steepest increase since for the same amount of mass they occupy the most volume. The data were fitted with Equation S2 to obtain the conversion constants, $k = 48 \pm 2$, 33 ± 1 , and 13.9 ± 0.2 for ULC, 1 mol% BIS, and 2.5 mol% BIS nanogels, respectively.

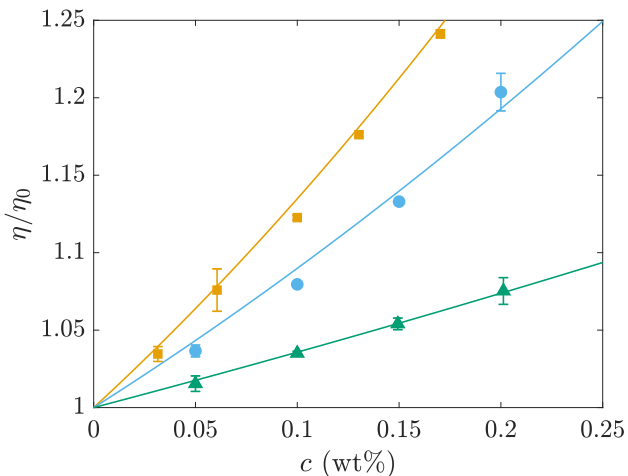


FIG. S3: Relative viscosity of nanogel suspensions as a function of concentration: ULC nanogels (orange squares), 1 mol% BIS microgels (blue circles), and 2.5 mol% BIS microgels (green triangles). Solid lines are fits with the Equation S2.

IV. MOLECULAR WEIGHT OF NANOGELS

Molecular weights of the nanogels, M_w , were calculated by combining the DLS and viscometry data as reported previously [12, 14]. In brief, by definition we can write $M_w = N_A \rho_{pol} v_{dry}$. The volume of a dry nanogel, v_{dry} , can be calculated from the viscometry conversion constant, k , according to the Equation S1, which gives:

$$M_w = N_A \frac{\rho_s v_{sw}}{k} \quad (S3)$$

where N_A is the Avogadro's number and v_{sw} is the volume of a swollen nanogel that is measured directly by DLS at 20 °C ($v_{sw} = \frac{4}{3}\pi R_h^3$). The molecular weights calculated in this study are listed in Table I of the main text and confirm that the ULC nanogels are the lightest.

V. EMULSION PREPARATION AND STABILITY

A. Variation of oil volume fraction in emulsions stabilised by ULC nanogels

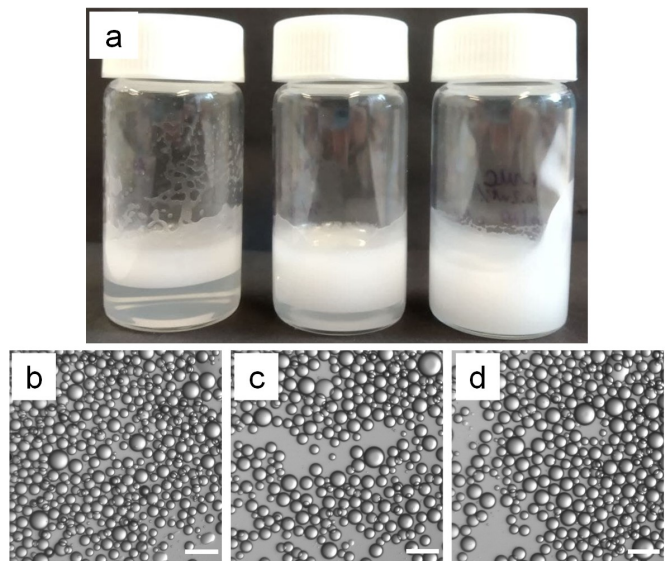


FIG. S4: (a) Photographs of emulsions stabilised by ULC nanogels as a function of n -decane volume fraction: (left to right) 30 vol%, 50 vol%, 70 vol%. (b-d) Corresponding optical micrographs (in the same order). Scale bar is 200 μm .

Emulsions stabilised with ULC nanogels were prepared at different volume fractions of n -decane (30 vol%, 50 vol%, and 70 vol%), while the concentration of ULC nanogels was kept constant (0.020 wt%). Creaming was observed at 30 and 50 vol% of decane, while at 70 vol% the emulsion remained homogeneous during storage (Figure S4 (a)). In all three cases, the emulsions flowed freely when the vial was tilted, *i.e.* no plug-flow was observed. Optical microscopy revealed no signs of droplet adhesion and flocculation, as can be seen in Figure S4 (b-d). The average size of the droplets did not depend significantly on the volume fraction of oil, which indicates that the concentration of ULC nanogels, rather than their number per unit volume of oil, determines the properties of the emulsion.

B. Flocculation of emulsion droplets for BIS-crosslinked nanogels

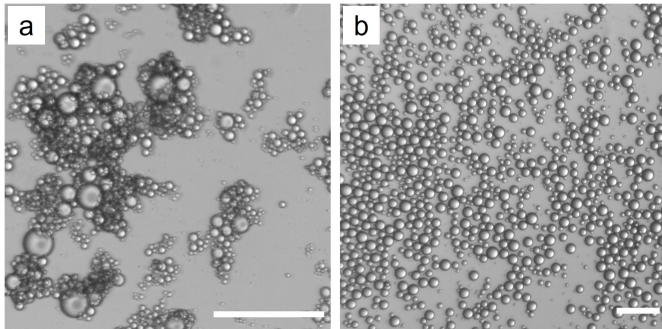


FIG. S5: Optical micrograph of emulsions stabilized by 2.5 mol% BIS nanogels at 0.06 wt% (a) and 3 wt% (b). Scale bar is 200 μm .

Unlike the ULC-nanogel-stabilized emulsions, emulsions stabilized with harder nanogels at low concentrations, in particular with 2.5 mol% BIS nanogels, consist of small strongly flocculated oil droplets, as can be seen in Figure S5 (a). However, this can be overcome by increasing the concentration of 2.5 mol% BIS nanogels to 3 wt%. In this case, big individual droplets were observed with no signs of flocculation.

The strong adhesion between droplets that results in flocculation has been explained in the literature by ‘bridging’ of adjacent droplets by nano- or microgels adsorbing at two interfaces simultaneously [15, 16]. This requires individual nanogels to protrude significantly from the surface into the aqueous phase [15]. However, the more the packing density of nano- or microgels at the droplet surface, the more their coronas are compressed and cores approach each other resulting in a more uniform layer that prevents such ‘bridging’ events. Higher packing densities, and consequently less flocculation, can be achieved by either increasing emulsification temperature [15] or microgel concentration [17]. The advantage of using ULC nanogels to stabilise emulsions is that already at low weight concentrations uniform coverage can be achieved.

C. Interfacial tension and dilatational rheology

To better understand the difference in emulsion-stabilising properties between linear pNIPAM, ULC nanogels, and BIS-crosslinked nanogels, we measured the interfacial dilatational moduli, E' and E'' , of the n -decane drop immersed in the respective aqueous solutions at $T = 20^\circ\text{C}$. First, we checked that spontaneous adsorption of nanogels leads to a decrease of interfacial tension (IFT), which was measured by the pendant drop method using a drop shape analyser Krüss DSA-100S. A drop of n -decane ($V = 18 \mu\text{L}$) was created in an aqueous solu-

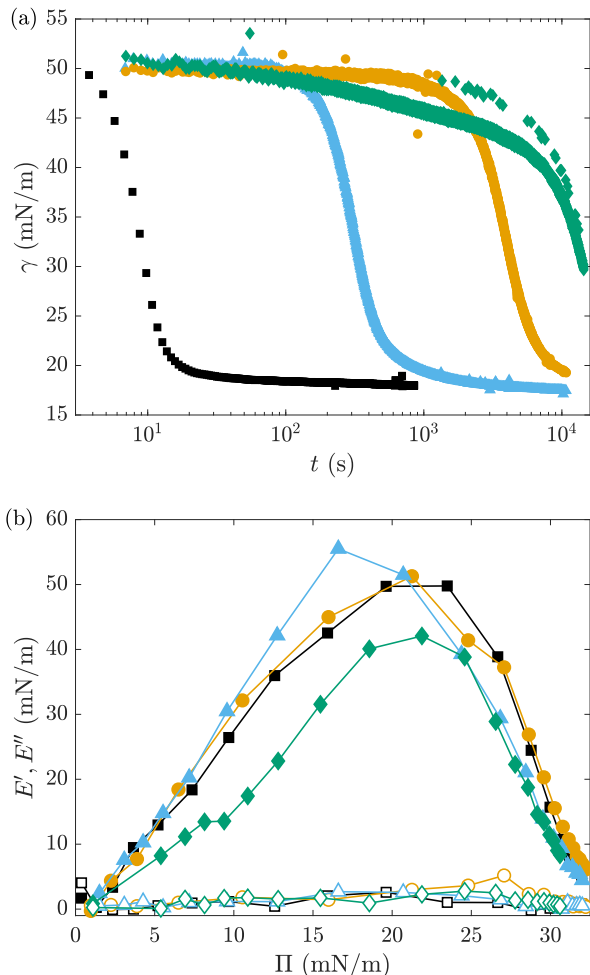


FIG. S6: (a) Interfacial tension between n -decane and an aqueous solution of linear pNIPAM (black squares), ULC nanogels (orange circles), 1% BIS nanogels (blue triangles), 2.5% BIS nanogels (green diamonds). (b) Dilatational moduli E' (filled symbols) and E'' (empty symbols) of the n -decane/water interface at $T = 20^\circ\text{C}$ as a function of surface pressure Π for linear pNIPAM (black squares), ULC nanogels (orange circles), 1% BIS nanogels (blue triangles), 2.5% BIS nanogels (green diamonds).

tion of nanogels or polymer and its shape was recorded as a function of time. Drop shapes were fitted with the Young-Laplace equation to obtain the interfacial tension using the Krüss Advance software. The interfacial tension reaches a value $\gamma = 18 \pm 1 \text{ mN/m}$ for both linear pNIPAM and nanogels independently of concentration. Figure S6(a) shows the IFT as a function of time at a fixed concentration $c = 0.005 \text{ wt}\%$. Adsorption kinetics slow down with increasing crosslinker content in agreement with previous studies [18, 19]. However, 1 mol% BIS nanogels do not follow this trend and adsorb faster compared to ULC nanogels at the same weight concentration. This fact is surprising, because 1 mol% BIS nanogels have

both higher molecular weight (consequently, lower number density in solution) and higher hydrodynamic radius compared to ULC nanogels (Table I). A possible explanation is the slight positive charge of these nanogels, which are electrostatically attracted to a negatively charged interface [20].

The viscoelastic properties of the interface were measured as a function of IFT or, equivalently, surface pressure of the monolayer $\Pi(t) = \gamma_0 - \gamma(t)$. The response of the interface is described by the complex dilatational modulus $E^* = d\gamma/d\ln A = E' + iE''$. The real and imaginary parts, corresponding to the storage and loss dilatational moduli, were calculated as $E' = |E^*| \cos \delta$ and $E'' = |E^*| \sin \delta$, respectively, where δ is the phase angle between the area A and the interfacial tension γ . The frequency was set to $f = 0.2$ Hz and oscillation amplitudes were within the linear viscoelastic regime. The values of E' and E'' are shown in Figure S6(b).

The values of the storage modulus, E' , of linear pNIPAM and all studied nanogels have similar values and follow a similar dependence on surface pressures with a maximum at $\Pi \simeq 15 - 20$ mN/m. The values of the loss modulus, E'' , were also similar for all systems and were always less than the elastic moduli, indicating a primarily elastic response of all monolayers. We note that the observed trends are in qualitative agreement with similar measurements of bigger pNIPAM microgels [21] and linear pNIPAM [22].

VI. CORRELATION BETWEEN 2D COMPRESSION STATES AND PACKING DENSITY OF ULC NANOGELES IN EMULSION

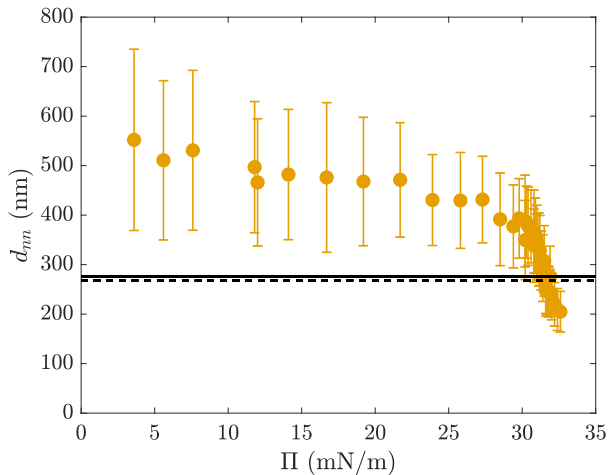


FIG. S7: Nearest-neighbour distances between ULC nanogels at a 2D decane-water interface obtained by Scotti *et al.* [7]. Solid line corresponds to the calculated nearest-neighbour distance between ULC nanogels in emulsion, as discussed in the main text. Dashed line corresponds to hydrodynamic diameter of ULC nanogels.

Figure S7 shows the nearest-neighbour distances vs. the surface pressure in Langmuir monolayers of ULC nanogels measured using gradient Langmuir-Blodgett deposition and AFM visualisation by Scotti *et al.* [7]. During the deposition, the barriers of the Langmuir trough were constantly moving and decreasing the total surface area of the trough. Therefore, nanogels at different compression states, corresponding to different surface pressures Π , were transferred onto the substrate in a single deposition experiment. The nearest-neighbour distance at different Π was calculated from AFM images in dry state, since it has been shown that the structure of the monolayer is preserved during drying [23, 24]. The solid line in Fig. S7 corresponds to the nearest-neighbour distance between ULC nanogels in emulsions, $d_{nn} = 276 \pm 7$ nm, calculated in this work. The dashed line shows the hydrodynamic diameter of ULC nanogels in solution for comparison.

-
- [1] A. Scotti, M. Brugnoli, C. G. Lopez, S. Bochenek, J. J. Crassous, and W. Richtering, Flow properties reveal the particle-to-polymer transition of ultra-low crosslinked microgels, *Soft Matter* **16**, 668 (2020).
- [2] C. G. Lopez and W. Richtering, Does flory–rehner theory quantitatively describe the swelling of thermoresponsive microgels?, *Soft Matter* **13**, 8271 (2017).
- [3] J. E. Houston, L. Fruhner, A. de la Cotte, J. Rojo González, A. Petrunin, U. Gasser, R. Schweins, J. Allgaier, W. Richtering, A. Fernandez-Nieves, and A. Scotti, Resolving the different bulk moduli within individual soft nanogels using small-angle neutron scattering, *Science Advances* **8**, eabn6129 (2022).
- [4] P. J. Flory and J. Rehner, Statistical mechanics of cross-linked polymer networks i. rubberlike elasticity, *J. Chem. Phys.* **11**, 512 (1943).
- [5] P. J. Flory and J. Rehner, Statistical mechanics of cross-linked polymer networks ii. swelling, *J. Chem. Phys.* **11**, 521 (1943).
- [6] A. Scotti, M. F. Schulte, C. G. Lopez, J. J. Crassous, S. Bochenek, and W. Richtering, How softness matters in soft nanogels and nanogel assemblies, *Chemical Reviews* **122**, 11675 (2022).
- [7] A. Scotti, S. Bochenek, M. Brugnoli, M. A. Fernandez-Rodriguez, M. F. Schulte, J. E. Houston, A. P. H. Gelissen, I. I. Potemkin, L. Isa, and W. Richtering, Exploring the colloid-to-polymer transition for ultra-low crosslinked microgels from three to two dimensions, *Nature Communications* **10**, 1418 (2019).
- [8] M. Stieger, W. Richtering, J. Pedersen, and P. Lindner, Small-angle neutron scattering study of structural changes in temperature sensitive microgel colloids, *J. Chem. Phys.* **120**, 6197 (2004).
- [9] M. F. Schulte, S. Bochenek, M. Brugnoli, A. Scotti, A. Mourran, and W. Richtering, Stiffness tomography of ultra-soft nanogels by atomic force microscopy, *Angewandte Chemie* **133**, 2310 (2021).
- [10] B. H. Zimm, The scattering of light and the radial distribution function of high polymer solutions, *The Journal of chemical physics* **16**, 1093 (1948).
- [11] H. Senff and W. Richtering, Temperature sensitive microgel suspensions: Colloidal phase behavior and rheology of soft spheres, *J. Chem. Phys.* **111**, 1705 (1999).
- [12] A. Scotti, U. Gasser, E. S. Herman, J. Han, A. Menzel, L. A. Lyon, and A. Fernandez-Nieves, Phase behavior of binary and polydisperse suspensions of compressible microgels controlled by selective particle deswelling, *Phys. Rev. E* **96**, 032609 (2017).
- [13] P. S. Mohanty, S. Nöjd, K. v. Gruijthuisen, J. J. Crassous, M. Obiols-Rabasa, R. Schweins, A. Stradner, and P. Schurtenberger, Interpenetration of polymeric microgels at ultrahigh densities, *Scientific Reports* **7**, 1487 (2017).
- [14] G. Romeo, L. Imperiali, J.-W. Kim, A. Fernández-Nieves, and D. A. Weitz, Origin of de-swelling and dynamics of dense ionic microgel suspensions, *The Journal of Chemical Physics* **136**, 124905 (2012).
- [15] M. Destribats, V. Lapeyre, E. Sellier, F. Leal-Calderon, V. Ravaine, and V. Schmitt, Origin and control of adhesion between emulsion drops stabilized by thermally sensitive soft colloidal particles, *Langmuir* **28**, 3744 (2012).
- [16] H. Monteillet, M. Workamp, J. Appel, J. M. Kleijn, F. A. Leermakers, and J. Sprakel, Ultrastrong anchoring yet barrier-free adsorption of composite microgels at liquid interfaces, *Advanced Materials Interfaces* **1**, 1300121 (2014).
- [17] L. Keal, V. Lapeyre, V. Ravaine, V. Schmitt, and C. Monteux, Drainage dynamics of thin liquid foam films containing soft pnipam microgels: influence of the cross-linking density and concentration, *Soft Matter* **13**, 170 (2017).
- [18] M. C. Tatry, E. Laurichesse, A. Perro, V. Ravaine, and V. Schmitt, Kinetics of spontaneous microgels adsorption and stabilization of emulsions produced using microfluidics, *Journal of colloid and interface science* **548**, 1 (2019).
- [19] Z. Li, K. Geisel, W. Richtering, and T. Ngai, Poly (n-isopropylacrylamide) microgels at the oil–water interface: adsorption kinetics, *Soft Matter* **9**, 9939 (2013).
- [20] R. Vácha, S. W. Rick, P. Jungwirth, A. G. de Beer, H. B. de Aguiar, J.-S. Samson, and S. Roke, The orientation and charge of water at the hydrophobic oil droplet–water interface, *Journal of the American Chemical Society* **133**, 10204 (2011).
- [21] F. Pinaud, K. Geisel, P. Massé, B. Catargi, L. Isa, W. Richtering, V. Ravaine, and V. Schmitt, Adsorption of microgels at an oil–water interface: correlation between packing and 2d elasticity, *Soft Matter* **10**, 6963 (2014).
- [22] B. Noskov, A. Akentiev, A. Y. Bilibin, D. Grigoriev, G. Loglio, I. Zorin, and R. Miller, Dynamic surface properties of poly (n-isopropylacrylamide) solutions, *Langmuir* **20**, 9669 (2004).
- [23] K. Geisel, W. Richtering, and L. Isa, Highly ordered 2d microgel arrays: compression versus self-assembly, *Soft Matter* **10**, 7968 (2014).
- [24] C. Picard, P. Garrigue, M.-C. Tatry, V. Lapeyre, S. Ravaine, V. Schmitt, and V. Ravaine, Organization of microgels at the air–water interface under compression: Role of electrostatics and cross-linking density, *Langmuir* **33**, 7968 (2017).